https://doi.org/10.15255/KUI.2020.084
KUI-37/2021
Original scientific paper
Received December 25, 2020
Accepted June 26, 2021

Recycling of Waste Expanded Polystyrene as an Effective Adsorbent of Naphthalene from Aqueous Solution

O. C. Taiwo,[a,b] *T. J. Afolabi*,[a,b] *F. N. Osuolale*,[a] *A. O. Ajani*,[a] *O. A. Aworanti*,[a] *O. R. Ogunleye*, [a,b] and *A. O. Alade*[a,b,c*]

[a] Department of Chemical Engineering, Ladoke Akintola University of Technology, Ogbomoso, Nigeria
[b] Bioenvironmental, Water and Engineering Research Group, (BWERG), Ladoke Akintola University of Technology, Ogbomoso, Nigeria
[c] Science and Engineering Research Group, (SEARG), Ladoke Akintola University of Technology, Ogbomoso, Nigeria

Abstract

Batch adsorption process factors [contact time (20–150 min), adsorbent dosage (0.5–1.5 g), adsorbate concentration (5–30 mg l^{-1}), and agitation rate (100–250 rpm)] were optimised based on D-optimal Design under the Response Surface Methodology (RSM) of the *Design-Expert Software* (7.6.8) for the removal of naphthalene from aqueous solution using adsorbent developed from Acetylated Waste Expanded Polystyrene (AWEPs). The maximum adsorption capacity (5.6608 mg g^{-1}) achieved was well fitted to Dubinin-Radushkevich Isotherm ($R^2 = 0.9949$). The SSE (< 0.05) and ARE (< 4.0 %) indicated pseudo-second-order as the most suitable model. This research has demonstrated the effectiveness of the WEPs for the removal of naphthalene from the aqueous solution.

Keywords

Adsorption, D-optimal, naphthalene, waste expanded polystyrene

1 Introduction

Polycyclic aromatic hydrocarbons (PAHs) are a class of organic compounds characterised by two or more fused benzene rings. They are carcinogenic, mutagenic, and toxic.[1] There are sixteen listed PAHs as priority pollutants that have been linked to various health challenges in humans.[2,3] PAHs are by-products of various anthropogenic and industrial activities, such as incomplete combustion of coal, fuel, garbage, oil, oil spillage, organic substances, polymers, refuse, tobacco smoke, and wood, among others.[4,5,6,7] The negative effect of PAHs in the environment has been a great concern to researchers[8] to mitigate their serious effects on the human body.[5,8,9]

PAHs have a strong resistance to biological degradation, and some conventional physicochemical processes have not demonstrated the desired potency for their removal.[5] However, adsorption processes, involving the use of activated carbon derived from synthetic, natural, and renewable sources have been deployed for the successful removal of PAHs.[5,8,10] This may not be unconnected to the advantages of the ease in operation, cost-effectiveness, and insensitivity to toxic substances compared to other separation techniques.[9] Activated carbon, commonly used in the adsorption process, has high adsorption capacities for a wide range of pollutants because of its porous microstructures and large surface areas.[11] However, the purchase cost and the cost of regeneration of AC are expensive,[12] besides there is 10–15 % loss during regeneration.[13] Adsorbents such as carbon nanotube, zeolite, diatomite, and organoclay have been used for the adsorption of PAHs from aqueous solutions.[14,15,16] Naphthalene is an important PAH that has a molecule containing two benzene rings[17] with molecular formula $C_{10}H_8$, obtainable from petroleum refining and coal tar distillation.[18] Its presence in the environment is more pronounced, relative to the other types of PAHs.[13] Some authors have used various types of adsorbent originated from clay, coal, and agricultural biomass for the removal of naphthalene from wastewater.[19,20,21,22]

Expanded polystyrene (EPS) are agglomerated small and expandable plastic "beads" used to produce food packages,[23] because of their calendaring surface, which prevents absorption of water, oil, beverages, and other processed food products. Used EPS has relatively low scrap value and is discarded after use.[24,25] Its non-biodegradable nature makes it persist in the environment and its build-up reduces the holding capacity of landfills or dumpsites.[26,27] Reuse of EPS for environmental remediation is reported in the works of *Gwenzi et al., Siyal et al., Alsewailem and Aljlil*, and *Ruziwa et al*.[26,27,28,29,30] This study aimed at recycling EPS waste into an effective adsorbent for the removal of naphthalene from the aqueous solution.

2. Experimental

2.1 Materials and sample preparation

WEPs, sourced from dumpsites were washed to remove oil and dirt from their surfaces. The collected WEPs were soaked in detergent solution and stirred until the strength

* Corresponding author: Abass Olanrewaju Alade, PhD
Email: aoalade@lautech.edu.ng

of the detergent became weak. They were then rinsed thoroughly with a copious amount of distilled water before being sun-dried and oven-dried at 105 °C to constant weight. They were reduced to relatively uniform sizes to reduce the impact of calendaring and expose the pores.[30] All the reagents used in this research were of analytical grade and used without further purification.[31]

[Acetic acid (γ: 60.052 g mol^{-1}, T_b: 118 °C, ρ: 1.05 g cm^{-3}, T_m: 16.6 °C, CAS 64-19-7), NaOH (γ: 39.997 g mol^{-1}, ρ: 2.13 g cm^{-3}, T_b: 1,388 °C, CAS 1310-73-2), Naphthalene (T_m: 80.26 °C, γ: 128.1705 g mol^{-1}, T_b: 218 °C, ρ: 1.14 g cm^{-3}, CAS 91-20-3), Ethanol (T_b: 78.37 °C, γ: 46.07 g mol^{-1}, T_m: −114.1 °C, Density: 789 kg m^{-3}, CAS 64-17-5)].

2.2 Activation of WEPs

The WEPs were mixed in 100 ml of acetic acid (c = 4.15 mol dm^{-3}) at a ratio of 1.5 : 1 (mass of activant/mass of precursor) and microwaved in the oven at 600 Hz for 90 min, the excess acid was boiled off. The pH of the acetylated WEPs (AWEPs) developed was neutralized with NaOH and oven-dried to constant weight.[28,30]

2.3 Characterisation of AWEPs

The ash and moisture contents were determined by the ASTM analytical method[32] and the method adopted by *Ekpete and Horsfall*.[33] The ash and moisture contents were calculated according to Eqs. (1) and (2).[31] Fourier Transform Infrared Spectroscopy (FTIR) was used to determine the functional group on the surface of AWEPs before and after adsorption. The samples were prepared with potassium bromide at a 1 : 10 ratio and pressed into the pelletized disc.[34] The FTIR spectrum of WEPs, AWEPs, and spent WEPs (SWEPs) adsorbents were recorded within the range of 400–4000 cm^{-1}.

$$\text{ash content}(\%) = \frac{m_1}{m_2} \cdot 100 \tag{1}$$

$$\%\ \text{moisture content} = \frac{m_4 - m_3}{m_5 - m_3} \cdot 100 \tag{2}$$

where m_1 is the mass of ash, m_2 is the mass of the dried sample, m_3 is the mass of crucible, m_4 is the mass of crucible with the wet sample, and m_5 is the mass of the crucible with the dry sample.

2.4 Batch adsorption

2.4.1 Adsorption studies

A stock solution of naphthalene of 200 mg l^{-1} was prepared by dissolving 200 mg of naphthalene in 100 ml of ethanol. Distilled water was added to make 1 l. The stock solution was further diluted with distilled water accordingly to produce the desired concentration.[35]

The study type used for this experimental design for the adsorption study was the Response Surface Methodology (RSM).[36] The initial design suggested by the *Design-Expert software* (7.6.8) was D-optimal. Zero (0) centre point was chosen for the design with no blocks selected, and a build time of 875 min was used for the design model. The factors are activant concentration (A), impregnation ratio (B), microwave time (C), and microwave frequency (D) while the response is adsorption capacity.[26,28] Determined amount (0.5–1.5 g) of AWEPs was mixed with 100 ml naphthalene solution of specific concentration (5–30 mg l^{-1}) and shaken on a rotary shaker at a specific agitation rate (100–250 rpm), and at room temperature (28±2 °C),[26,28] according to the D-optimal Design (Table 1). The mixture was centrifuged and the supernatant was analysed using UV-Spectrometer (UV-6100A, manufacturer: METASH A-MATRIX) at a wavelength of 275 nm.[37] Different concentrations (5–50 mg l^{-1}) of naphthalene were prepared earlier, and UV-Spectrometer (UV-6100A) at a wavelength of 275 nm was used to their corresponding absorbances, which were used to develop the calibration curve from which the equation for evaluating the naphthalene concentration from absorbance was determined. The adsorption capacity and removal efficiency were evaluated by Eqs. (3) and (4).

$$\text{adsorption capacity}\left(\frac{\text{mg}}{\text{g}}\right) = \frac{(\gamma_o - \gamma_t)V}{m} \tag{3}$$

$$\text{removal}(\%) = \frac{\gamma_o - \gamma_f}{c_o} \tag{4}$$

where γ_o (mg l^{-1}) is the initial concentration of naphthalene solution in contact with adsorbent, γ_t (mg l^{-1}) is the final concentration of naphthalene solution after the batch adsorption procedure at any time t, m (g) is the mass of adsorbent, and V (l) is the volume of the naphthalene in solution.

Table 1 – Range of selected factors for naphthalene adsorption

Activation factors	Unit	Ranges	
		Low	High
naphthalene concentration	mg l^{-1}	5.0	30.0
dosage	g	0.5	1.5
time	min	30	60
agitation rate	rpm	100	250

2.4.2 Effect of adsorption factors

The optimum conditions for the adsorption of naphthalene using AWEPs was subjected to OFAT procedures during which the effects of contact time and concentration were investigated when one of the factors was varied at a time.[38,39,40]

2.5 Investigation of suitable adsorption isotherms

The adsorption data obtained were fitted to selected isotherm models. Their constants were evaluated, and the

correlation coefficient (R^2) was used to express the extent of correlation between the experimental data and the model predicted values.[41]

2.5.1 Langmuir isotherm model

The Langmuir isotherm model is expressed by Eq. (5) and the linear form Eq. (6) was used to generate the plot of $\frac{\gamma_e}{q_e}$ against γ_e, which gave a straight-line graph with a slope $\frac{1}{q_m}$ and intercept of $\frac{1}{q_m K_L}$.

$$q_e = \frac{q_m K_L \gamma_e}{1 + K_L \gamma_e} \tag{5}$$

$$\frac{\gamma_e}{q_e} = \frac{1}{q_m K_L} + \frac{\gamma_e}{q_m} \tag{6}$$

where q_e is the adsorption capacity at equilibrium (mg g^{-1}), γ_e is the equilibrium concentration of the adsorbate solution (mg l^{-1}), K_L is the constant related to the free energy of adsorption (l mg^{-1}), and q_m is the maximum adsorption capacity at monolayer coverage (mg g^{-1}).

2.5.2 Freundlich isotherm model

The Freundlich isotherm model equation, Eq. (7), assumes a heterogeneous adsorbent surface with its adsorption sites at varying energy levels. Its linear form Eq. (8) was used to generate the plot of $\ln q_e$ against $\ln \gamma_e$ that is needed to determine the Freundlich constants (k_F, and $1/n$).[42]

$$q_e = k_F \gamma_e^{\frac{1}{n}} \tag{7}$$

$$q_e = \frac{1}{n} \ln \gamma_e + \ln k_F \tag{8}$$

where k_F is the Freundlich constant, and q_e is the adsorption capacity at equilibrium (mg g^{-1})

2.5.3 Temkin isotherm model

Temkin isotherm model explicates that the adsorbate-adsorbent interactions and the related change in heat and/or energy of adsorption are assumed to be linear ---+-characterised by a uniform distribution of binding energy and up to some maximum binding energy.[42] Such an assumption cannot hold for a logarithmic relationship. The Temkin isotherm model is expressed by Eq. (9), while its linear form is expressed by Eq. (10), and was further simplified to Eq. (11).

$$q_e = \frac{RT}{b} \ln(A \gamma_e) \tag{9}$$

$$q_e = \frac{RT}{b} \ln A + \frac{RT}{b} \log \gamma_e \tag{10}$$

$$q_e = B \ln A + B \ln \gamma_e \tag{11}$$

where $B = RT/b$, B is the molecular interaction parameter related to the heat of adsorption. A and B are the Temkin isotherm constants, T (K) is the absolute temperature, and R is the ideal gas constant (8314 J mol^{-1} K^{-1}).

2.5.4 Dubinin-Radushkevich isotherm

Dubinin-Radushkevich (D-R) isotherm Eq. (12) assumes that pore filling influenced the adsorption mechanism in micropores and not a layer-by-layer formation of a film in the walls of the adsorbent pores.[43] The linear form of the D-R isotherm equation is expressed in Eq. (13) and was used to plot $\ln q_e$ against ε^2 needed to determine the q_m and β from the intercept and slope.

$$q_e = q_m e^{-\beta \varepsilon^2} \tag{12}$$

$$\ln q_e = \ln q_m - \beta \varepsilon^2 \tag{13}$$

where β (KJ^2 mol^2) is the free energy of sorption per mole of the naphthalene as it migrates to the surface of WEPs from an infinite distance in the solution, q_m is the maximum adsorption capacity, and ε is the Polanyi potential (J mol^{-1}), which is expressed by Eq. (14):

$$\varepsilon = RT \ln\left(1 + \frac{1}{\gamma_e}\right) \tag{14}$$

where R is the universal gas constant (8.314 J mol^{-1} K^{-1}), T is the absolute temperature (K), and γ_e is the equilibrium concentration of naphthalene.

2.6 Adsorption kinetics studies

The pseudo-first-order model, pseudo-second-order model, and intraparticle diffusion model were employed to evaluate the experimental data generated in this study.

2.6.1 Pseudo-first-order model

This model (Eq. (15)) is based on a solid capacity and its plot of $\ln(q_e - q_t)$ *vs* t that gives a straight line from which K_1 and q_t were evaluated based on the slope and intercept.

$$\ln(q_e - q_t) = \ln q_t - K_1 t \tag{15}$$

where q_e is the equilibrium adsorption capacity (mg g^{-1}), q_t is the adsorption capacity at time (mg g^{-1}), K_1 is the pseudo-first-order rate constant (l min^{-1}), and t is the time taken.

2.6.2 Pseudo-second-order model

This model (Eq. (16)) was used to plot t/q_e *vs* t, which gave a straight line from which q_e and K_2 were evaluated.

$$\frac{t}{q_t} = \frac{1}{q_e K_2} + \frac{t}{q_e} \quad (16)$$

where K_2 is the rate constant of pseudo-second-order adsorption (g mg^{-1} min^{-1}).[43]

6.3 Intraparticle diffusion model

This model indicates that the rate-limiting step is the transport of the solute from the bulk of the solution to the adsorbent pores through the intraparticle process. It was expressed according to Eq. (17):[44]

$$q_t = k_{diff} t^{\frac{1}{2}} + C \quad (17)$$

where k_{diff} is the intraparticle diffusion rate constant (mg g^{-1} min$^{-0.5}$), t is time, and C is constant.

2.7 Test of the kinetics model

The impact of various error functions on the predicted isotherm parameters was analysed to determine the order of suitability of the selected isotherm models. Error functions such as Average Relative Error (ARE) and Sum of Error Square (SSE) were calculated according to the Eqs. (16) and (17).[45,46]

$$ARE = \frac{100}{n} \sum_{i=1}^{n} \left| \frac{q_{e,exp} - q_{e,cal}}{q_{e,exp}} \right| \quad (16)$$

$$SSE = \sum_{i=1}^{n} \frac{\left(q_{e,cal} - q_{e,exp}\right)^2}{n} \quad (17)$$

where $q_{e,exp}$ is the adsorption capacity at equilibrium experimental (mg g^{-1}), $q_{e,cal}$ is the adsorption capacity at equilibrium calculated (mg g^{-1}), and n is the number of data points.

3 Results and discussion

3.1 Physicochemical analysis of the adsorbent

There was a significant difference in the ash content between the WEPs (0.10 %) and AWEPs (0.39 %) (Table 2). This may be due to the impact of the activant on the composition of the untreated WEPs, and this further suggested that the activation process was evident.[47,48] The moisture content of AWEPs (14.82 %) was higher than that of WEPs (0.90 %), and this may be due to the soaking step during the activation process.

Table 2 – Proximate analysis of WEPS and AWEPS

Sample	Ash content / %	Moisture content / %
WEPs	0.10	0.90
AWEPs	0.39	14.82

WEPs – Waste Expanded Polystyrene, AWEPs – Acetylated Waste Expanded Polystyrene

3.2 FTIR characterisation of WEPs and AWEPs

The IR peaks observed in the WEPs ranged from 623.1 cm^{-1} to 3933.4 cm^{-1} and the peak height ranged from 21.8 cm^{-1} to 36.9 cm^{-1} (Fig. 1a). AWEPs had IR peaks that ranged from 613.7 cm^{-1} to 3892.3 cm^{-1} and peak height ranged from 3.5 cm^{-1} to 21.8 cm^{-1}. The IR peak for the spent SAWEPs ranged from 618.5 cm^{-1} to 3930.4, while the peak height ranged from 10 cm^{-1} to 27.4 cm^{-1}. The IR peaks observed in the WEPs shifted from (623.1–3933.4 cm^{-1}) to (613.7–3892.3 cm^{-1}) on AWEPs. All these changes suggested the impact of acetic acid activation on the surface improvement of the WEPs. The aromatic C−H band present in both WEPs and AWEPs is attributed to the presence of an aromatic benzene ring that is not split by the acidic modification on the WEPs. C−C−O at 1332 cm^{-1} was found in WEPs but disappeared in AWEPs due to the modification by acetic acid. These bands indicate the possible involvement of these functional groups on the surface of AWEPs in the naphthalene adsorption process.[47] WEPs and AWEPs surface chemistry were found to be different as some of the functional groups such as O−H and C−C−O disappeared due to the activation process.[48]

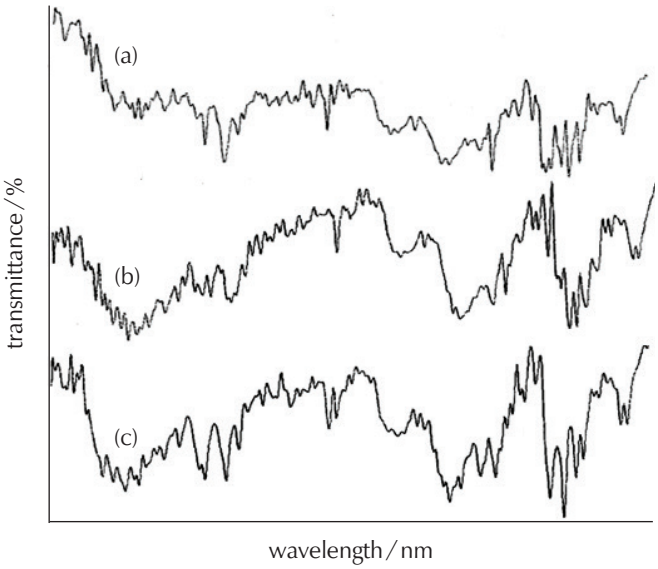

Fig. 1 – FTIR spectra for (a) Waste Expanded Polystyrene, (b) Acetylated Waste Expanded Polystyrene, and (c) Spent Acetylated Waste Expanded Polystyrene

3.3 Design summary for the adsorption capacity of AWEPs for naphthalene

Run 4 (60 min, 100 rpm, 5 mg l^{-1}, and 1.5 g) gave the lowest adsorption capacity (0.1623 mg g^{-1}), while Run 3 (30 min, 100 rpm, 30 mg l^{-1}, and 0.5 g) gave the highest adsorption capacity (5.6608 mg g^{-1}) (Table 3), which

Table 3 – Results of responses from adsorption experimental data

Run	Factors				Response
	A: time / min	B: agitation rate / rpm	C: concentration / mg l^{-1}	D: dosage / g	adsorption capacity / mg g^{-1}
1	30.00	100.00	17.50	1.50	0.6188
2	45.00	250.00	30.00	1.50	0.7565
3	30.00	100.00	30.00	0.50	5.6608
4	60.00	100.00	5.00	1.50	0.1623
5	30.00	100.00	5.00	0.50	0.4869
6	60.00	100.00	30.00	1.50	1.4231
7	30.00	250.00	5.00	1.50	0.3072
8	30.00	250.00	17.50	0.50	2.8130
9	60.00	100.00	17.50	0.50	2.9000
10	30.00	175.00	30.00	1.50	1.3072
11	60.00	250.00	5.00	0.50	0.9217
12	60.00	100.00	30.00	1.50	1.3072
13	30.00	100.00	30.00	0.50	3.0521
14	60.00	250.00	17.50	1.50	0.5898
15	60.00	250.00	30.00	0.50	4.4434
16	60.00	175.00	17.50	1.00	0.4065
17	30.00	250.00	5.00	1.50	1.9608
18	45.00	250.00	17.50	1.00	0.9717
19	60.00	250.00	30.00	0.50	4.7043
20	30.00	100.00	5.00	0.50	0.9838
21	30.00	175.00	17.50	1.00	0.4500
22	45.00	100.00	17.50	1.00	1.3630
23	45.00	175.00	23.75	1.00	2.2489
24	45.00	175.00	5.00	1.00	0.3304
25	30.00	250.00	30.00	1.00	2.2217

is higher than adsorption capacity of 1.44, 1.595, 1.527, and 4.39 mg g^{-1}, reported by *Ania et al.*,[49] *Murilo et al.*,[10] and *Alade et al.*,[8] for activated carbons, activated clay, and flamboyant pod activated carbon studied for the removal of naphthalene. A quadratic model was selected for this study because of its least standard deviation (10.33) and high R^2 (0.9835). The R^2 (0.9548) was very close to the adjusted R^2 of 0.9548, with less than 0.2 differences, as normally expected.[44] This indicated no large block effect nor any possible problem with the model and data obtained.[50] Adequate Precision, which measures the signal-to-noise ratio of the data, was 28.793, which was greater than the desired value (4.0), thus making the developed model very suitable to navigate the design space.[51]

3.4 Analysis of variance (ANOVA) for adsorption capacity of AWEPs

Prob> F of any term or model, less than 0.05, at a 95 % confidence interval is taken as significant.[31] The model F-value of 34.16 implies the model is significant and it has about 0.01 % chance of occurrence due to noise. Thus, C, AB, AC, AD, BC, BD, and CD are significant model terms (Table 4). The "Lack of fit F-value" of 0.63 implies the Lack of fit is not significant relative to the pure error, which makes the model fit[31] and there is a 62.61 % chance that a "Lack of fit F-value" this large could occur due to noise. This is further illustrated by Fig. 2, showing the effects of the model terms concerning Normal % probability. The points are distributed on the normal line starting from approximately 2 to 97 % on normal percentage distribution, Y-axis, and −1.5 to 2.5 on internally studentized residuals, X-axis though there is a stacking of the points.[31]

Table 4 – ANOVA for the Model and selected factors

Source	Sum of squares	D_f	Mean square	F value	P-value Prob >F
Model	51038.03	14	3645.57	34.16	< 0.0001*
A – time	14.27	1	14.27	0.13	0.7240
B – agitation rate	25.36	1	25.36	0.24	0.6390
C – concentration	5903.74	1	5903.74	55.32	< 0.0001*
D – dosage	113.17	1	113.17	1.06	0.3332
AB	2923.37	1	2923.37	27.39	0.0008*
AC	7680.27	1	7680.27	71.97	< 0.0001*
AD	1786.01	1	1786.01	16.74	0.0035*
BC	8533.81	1	8533.81	79.97	< 0.0001*
BD	1517.79	1	1517.79	14.22	0.0055*
CD	5305.82	1	5305.82	49.72	0.0001*
A^2	39.15	1	39.15	0.37	0.5615
B^2	0.21	1	0.21	$1.939 \cdot 10^{-3}$	0.9660
C^2	37.79	1	37.79	0.35	0.5683
D^2	69.13	1	69.13	0.65	0.4442
Residual	853.71	8	106.71		
Lack of fit	234.40	3	78.13	0.63	0.6261
Pure error	619.32	5	123.86		
Cor total	51891.75	22			

* Significant at $p < 0.05$

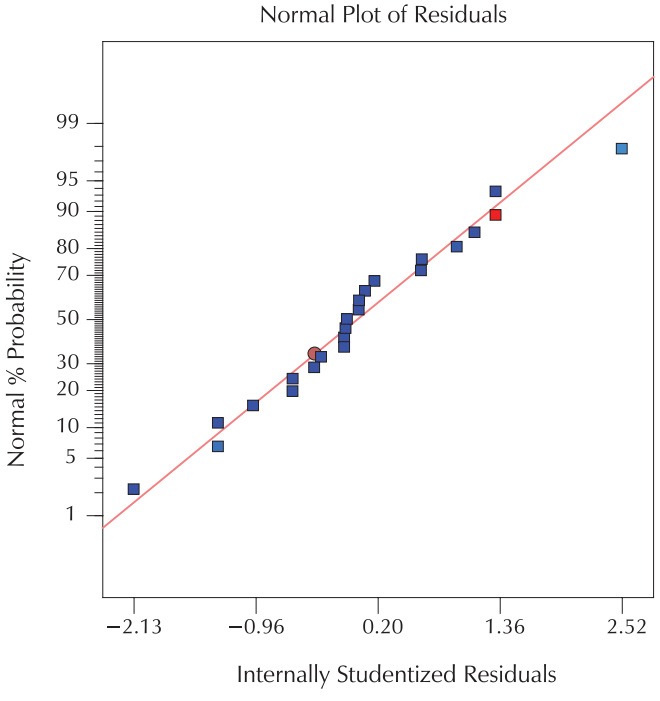

Fig. 2 – Effects of the model terms with respect to normal % probability

3.5 Model equation

The model equations, (Eqs. (18) and (19)), show the relationship between the adsorption capacity and the selected factors that can be used to predict the naphthalene adsorption. Model terms B, D, AD, B^2, A^2, C^2, and D^2 have positive coefficients, which indicate an increase in the adsorption capacity of AWEPs in the factors. The negative coefficients as observed in A, C, AB, AC, BD, CD, and B^2 indicate an antagonistic influence of these factors on the adsorption capacity of naphthalene. The empirical model equations in terms of coded factors are given in Eq. (18), for the significant and non-significant terms.

$$\begin{aligned}(\text{adsorption capacity})^{-3} = {} & +3.01 - 1.83A + \\ & + 2.46B - 25.23C + 6.27D - 30.38AB - \\ & - 31.98AC + 24.36AD + 33.65BC - 22.59BD - \\ & - 24.79CD + 8.26A^2 - 0.6B^2 + 7.35C^2 + 19.45D^2\end{aligned} \quad (18)$$

A B, C, and D are the coded variables for activant concentration, IMR, microwave time, and frequency, respectively.

3.6 Model graph for the selected factors on adsorption capacity for naphthalene

The plot of agitation rate with time (Fig. 3) shows a gradual decrease in adsorption capacity before a steep slope moving upward, and this indicates that the two factors cause a decrease, and then finally increase the adsorption rate. There is a slight decrease in the slope of concentration against time before (Fig. 4) and thus, means that the

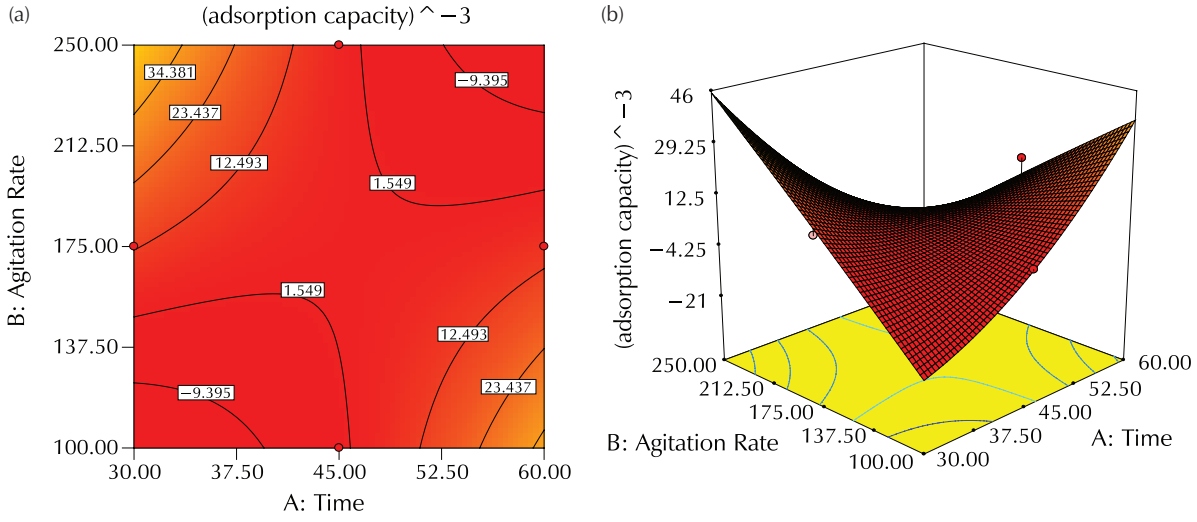

Fig. 3 – (a) Contour plot, and (b) 3D plot showing the relationship between time and agitation rate

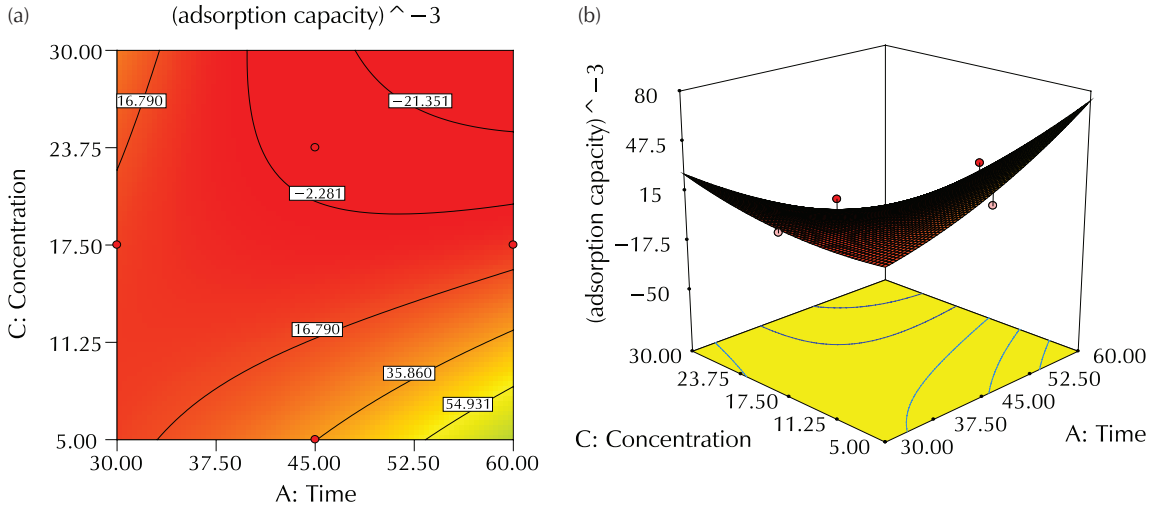

Fig. 4 – (a) Contour plot, and (b) 3D plot showing the relationship between time and concentration

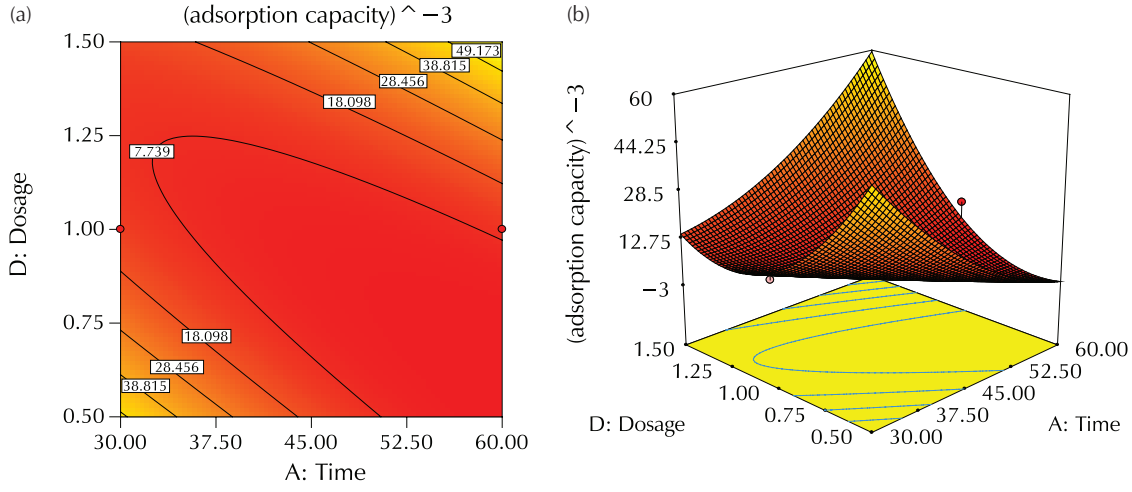

Fig. 5 – (a) Contour plot, and (b) 3D plot showing the relationship between dosage and time

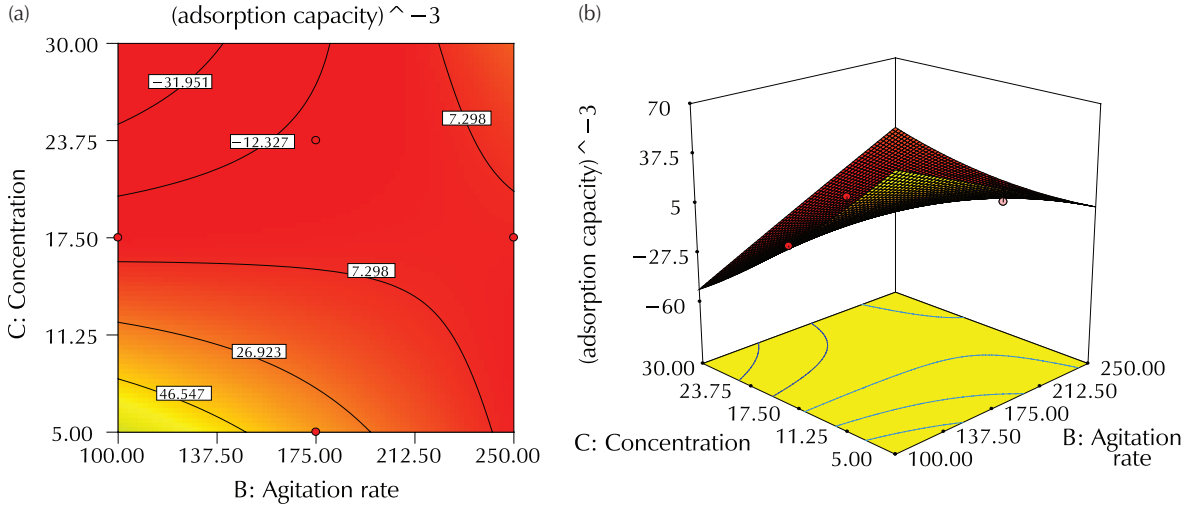

Fig. 6 – (a) Contour plot, and (b) 3D plot showing the relationship between concentration and agitation rate

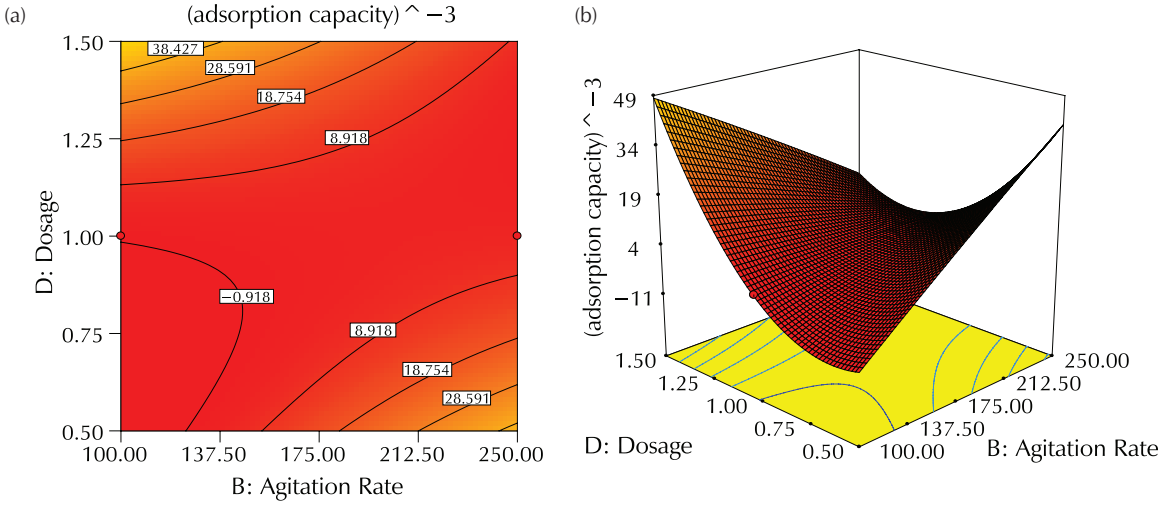

Fig. 7 – (a) Contour plot, and (b) 3D plot showing the relationship between dosage and agitation rate

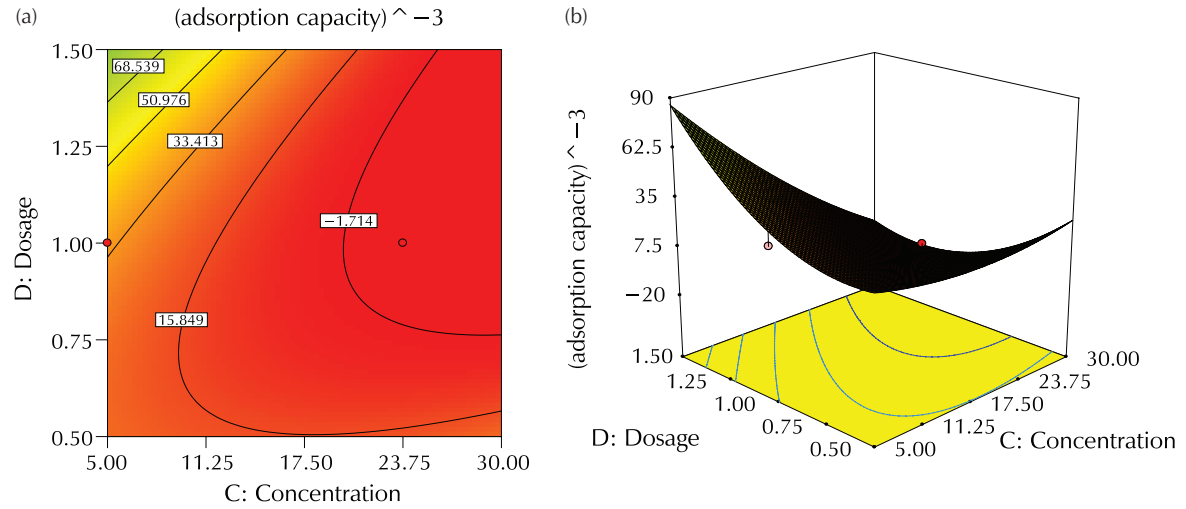

Fig. 8 – (a) Contour plot, and (b) 3D plot showing the relationship between dosage and concentration

lower value of these factors decreases the adsorption rate. Contrary to Figs. 3 and 4, there is a parabolic curve, an increase in adsorption capacity in the plot of dosage and time (Fig. 5). Further increase in dosage value with time caused a decrease in adsorption capacity (Fig. 6). Concentration against the agitation rate plot shows an increase in adsorption capacity (Fig. 4). Other factors that increased the adsorption rate were the dosage value and agitation rate (Fig. 7), but the contrary result was experienced in Fig. 8, in which the dosage and concentration decreased with the adsorption rate.

3.7 Numerical optimisation studies on adsorption capacity

Numerical optimisation was obtained from the software. The four factors (time, agitation rate, concentration, and dosage) were all set to "is in range" (Table 4), while the adsorption capacity was set to "maximise" with its upper and lower limit, respectively. The desirability values were 0.994, and the optimum values suggested by the software were 60 min, 100 rpm, 5 mg l^{-1}, and 1.5 g for time, agitation rate, concentration, and dosage, respectively (Fig. 9).

Table 5 – Selected factors used for optimisation showing their respective ranges

Name	Goal	Lower Limit	Upper Limit
time	is in range	30	60
agitation rate	is in range	100	250
concentration	is in range	5	30
dosage	is in range	0.5	1.5
(adsorption capacity) ^ −3	maximise	0.00551244	233.908

3.8 Effect of concentration on adsorption of naphthalene

An increase in the adsorbate initial concentration (10–30 mg l^{-1}) leads to an increase in the adsorption capacity (1.921–5.9217 mg g^{-1}) of the adsorbent due to the increase in the driving force of the concentration gradient (Fig. 10a). The adsorption of naphthalene was rapid at the initial stage of the contact time (30 min) for all the concentrations. This was because, in the beginning, all active sites on the adsorbent were vacant, hence, adsorption proceeded at a faster rate. After this, the rates of adsorption and desorption tended to be equal, and the extent of adsorption reduced and eventually became almost constant at equilibrium.[51] The percentage of removal also increased with increasing time for all the concentrations (Fig. 10b).

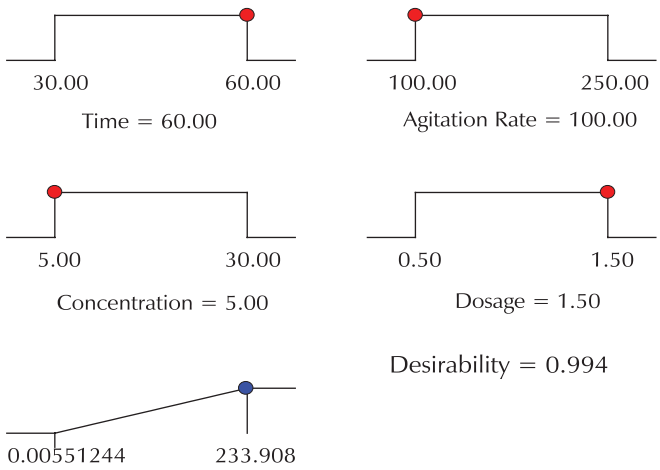

Fig. 9 – Graphical representation of the numerical optimisation

3.9 Effect of dosage on the adsorption of naphthalene

An increase in adsorbent dosage (0.5–2.5 g) led to a reduction (5.5739–1.1930 mg g^{-1}) in adsorption capacity (Fig. 11a), because of the effect of partial aggregation of naphthalene on the adsorbent surface, resulting in a decrease in total surface area available for naphthalene molecules. An increase in the adsorbent dosage increased the removal efficiency of naphthalene from 92.9 % to 99.4 %

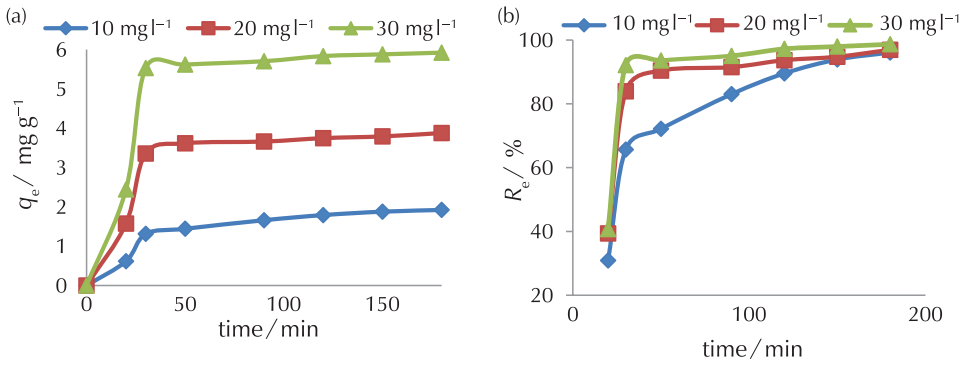

Fig. 10 – Effect of concentration on (a) adsorption capacity, and (b) removal efficiency

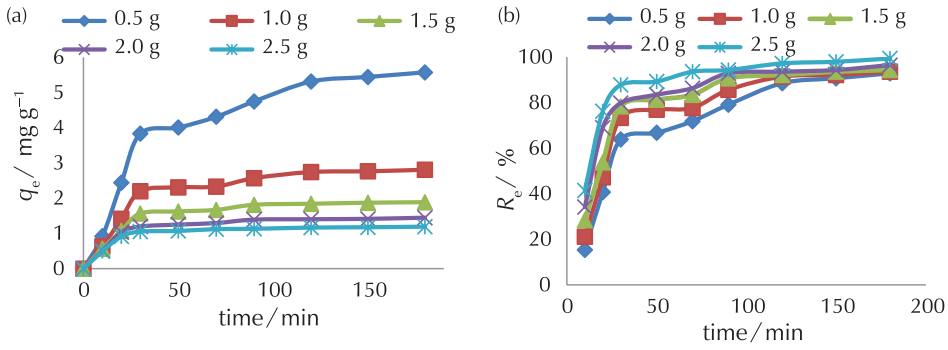

Fig. 11 – Effect of adsorbent dosage on (a) adsorption capacity, and (b) removal efficiency

at 180 min, due to the availability of more adsorption sites on the adsorbent (Fig. 11b).[52,53]

3.10 Adsorption isotherm study

3.10.1 Langmuir isotherm model

The values of q_m and K_L for AWEPs (Fig. 12) were −8.7108 mg g^{-1} and −0.1106, respectively. The low value of R^2 (0.4238) indicated that the experimental equilibrium data were not well described by the Langmuir model. The maximum adsorption capacity (q_m) obtained from this research (−8.7108 mg g^{-1}) (Table 5), was lower for the adsorption of naphthalene onto mesoporous molecular sieves, zeolite, Mesoporous organosilica, and banana peel activated carbon, respectively.[10,54]

3.10.2 Freundlich isotherm model

The Freundlich model to estimate K_f and $1/n$ are −0.0511 l mg^{-1} and 0.8059 from its intercepts and the slope, respectively (Fig. 13). The values of $1/n$ ranging from 0 to 1, indicates the model's favourability for the adsorption process,[55] and this value is lower than the previous research, except 0.7986 derived by *Gupta and Gupta*.[57] The negative K_f value obtained from this study was lower than

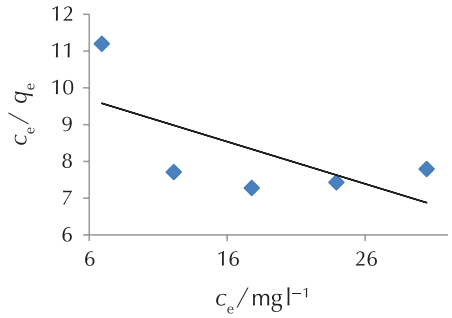

Fig. 12 – Plot of c_e/q_e against c_e for the effect of concentration

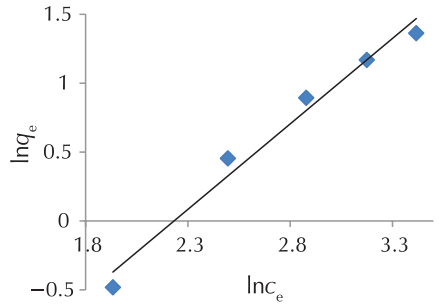

Fig. 13 – Plot of lnq_e against lnc_e for the effect of concentration

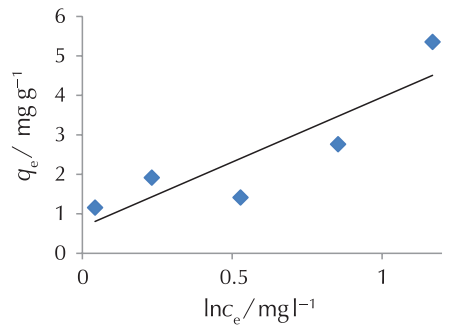

Fig. 14 – Plot of q_e against lnc_e for the effect of concentration

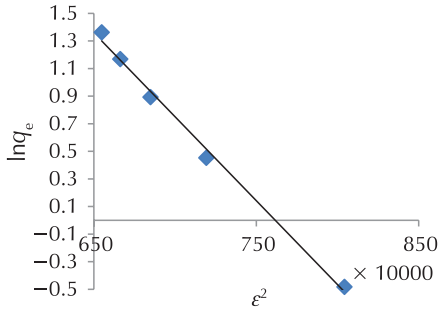

Fig. 15 – Plot of lnq_e against ε^2 for the effect of concentration

Table 6 – Comparison of Langmuir and Freundlich Isotherm Parameter to other studies

Adsorbent	Langmuir parameter	Freundlich parameters		Author
	q_m / mg g^{-1}	K_f	1/*n*	
Mesoporous Molecular Sieves	0.10624	NR	NR	*Murilo et al.* (2004)[10]
Zeolite	0.769	4.215	1.074	*Chang et al.* (2004)[56]
Mesoporous Organosilica	0.0466	0.227	0.97	*Carla et al.* (2011)[54]
Banana Peel Activated Carbon	NR*	21.54	0.7986	*Gupta and Gupta* (2015)[57]
AWEPS	−8.7108	−0.0511	0.8059	This study

*NR – not reported

the K_f value derived by *Carla et al.*,[54] *Chang et al.*,[56] *Gupta and Gupta*,[57] respectively. The R^2 (0.9777) was relatively high, thus making the Freundlich isotherm a better model compared to the Langmuir (0.4238) (Table 5).

3.10.3 Temkin isotherm model

Estimated Temkin isotherm parameters A and B were 6.0670 l g^{-1} and 1.2408 J mol^{-1}, respectively, (Fig. 14), with an R^2 value of 0.9883, which is higher than the R^2 values of 0.4238 and 0.9777 obtained for Freundlich and Langmuir, suggesting that the data better fitted Temkin isotherm than the other two.

3.10.4 Dubinin-Radushkevich isotherm for the effect of concentration

The Dubinin-Radushkevich isotherm model is described by the plot of lnq_e against E^2 (Fig. 15) and the estimated parameters, q_m and β are 25.1851 mg g^{-1} and 1 · 10^6 KJ^2 mol^2, respectively.

The mean free energy of biosorption β determines the biosorption mechanism as either a physical or chemical process. The biosorption process is chemically driven if the value of β is greater than 8 KJ^2 mol^2, but involves physical mechanism if less. The value obtained in this study indicated that the adsorption of naphthalene onto AWEPs was driven by a chemical process. The R^2 value was 0.9949, which was the highest of all the isotherm models investi-

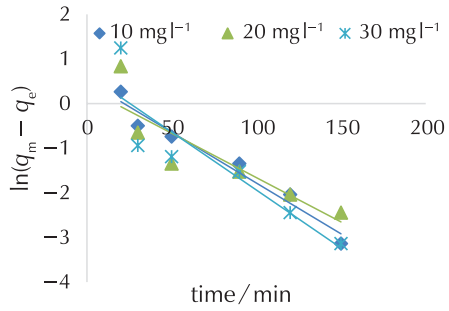

Fig. 16 – Plot of ln(q_m-q_e) against time for the effect of concentration

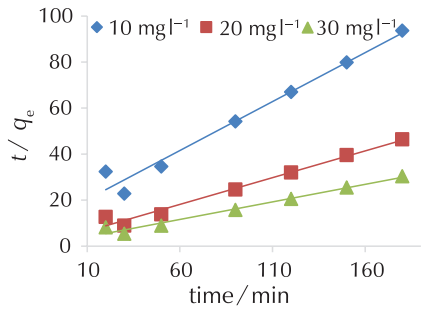

Fig. 17 – Plot of t/q_e against time for the effect of concentration

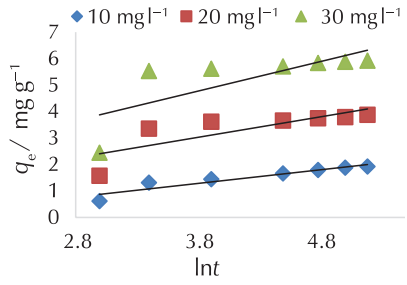

Fig. 18 – Plot of q_e against ln*t* for the effect of concentration

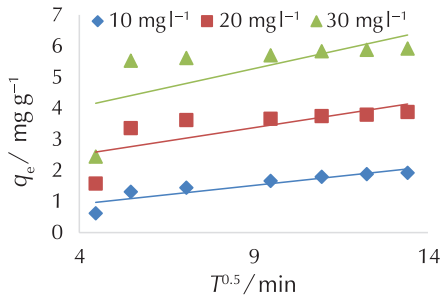

Fig. 19 – Plot of q_e against $T^{0.5}$ for the effect of concentration

gated, thereby giving the order of suitability as Langmuir < Freundlich < Temkin < Dubinin-Radushkevich isotherm. Therefore, Dubinin-Radushkevich isotherm model best fits the experimental data generated for the adsorption of naphthalene on AWEPs.

3.11 Investigation of adsorption kinetics

3.11.1 Pseudo-first-order kinetics model

The estimated k_1 values of 0.023, 0.020, and 0.026 had no visible trend (Fig. 16, Table 7). There is a wide disparity between the calculated equilibrium adsorption capacity $q_{e,calc}$, and the experimental equilibrium adsorption capacity ($q_{e,exp}$) values, contrary to a good correlation expected.[58] This suggests that the adsorption of naphthalene onto AWEPs does not fit the first-order kinetics. The R^2 for 10, 20, and 30 mg l^{-1} are 0.9609, 0.7838, and 0.8034, respectively and are relatively high.[31]

Table 8 – Kinetic parameters obtained for the kinetics models

Kinetics model	Parameters	10 mg l^{-1}	20 mg l^{-1}	30 mg l^{-1}
Pseudo-first order	$q_{e,cal}$ / mg g^{-1}	1.648	1.389	1.933
	$q_{e,exp}$ / mg g^{-1}	1.922	3.878	5.922
	K_1 / min^{-1}	0.023	0.020	0.026
	R^2	0.9609	0.7838	0.8034
Pseudo-second order	$q_{e,cal}$ / mg g^{-1}	2.349	4.297	6.545
	$q_{e,exp}$ / mg g^{-1}	1.922	3.878	5.922
	K_2 / g mg^{-1} min^{-1}	0.011	0.013	0.010
	R^2	0.9750	0.9804	0.9785
Elovich	A	0.140	0.872	1.816
	B	1.951	1.298	0.900
	R^2	0.8905	0.6349	0.5503
Intraparticle diffusion	K_{id}	0.120	0.172	0.246
	C	0.434	1.821	3.060
	R^2	0.8194	0.5322	0.4504

3.11.2 Pseudo-second-order kinetics model for the effect of concentration

The $q_{e.\ cal}$ obtained from the plot of t/q_e *vs* t (Fig. 17) were 2.349, 4.297, and 6.545 mg l^{-1}, showing a direct relationship with the increase in concentration. The values of $q_{e.cal}$ were relatively closer to the values of $q_{e,exp}$. The values of K_2 (0.011, 0.013, and 0.010 g mg^{-1} min^{-1}) had no particular pattern with increasing concentration. The R^2, (0.9750, 0.9804, and 0.978) were higher than the R^2, obtained for the first-order model (Table 7).

3.11.3 Elovich kinetic model

The plot of q_e against ln$t$ for Elovich kinetic model (Fig. 18) gave the values of initial adsorption rate, α as 0.14, 0.872, and 0.814, while the rate of surface coverage, β, were 1.951, 1.298, and 1.900 for 10, 20 and 30 mg l^{-1}, respectively. The R^2 (0.8905, 0.6349, and 0.5503) displayed an inverse relation with the initial concentration. The increasing order of suitability of the kinetic models, based on R^2 obtained, was Elovich < pseudo-first-order < pseudo-second-order kinetic model. Therefore, the adsorption experiment of naphthalene onto AWEPs is best described by the pseudo-second-order kinetic model.

3.11.4 Intraparticle diffusion model

The kinetic parameter (C) obtained from the plot of q_e against $t^{\frac{1}{2}}$ (Fig. 19) was 0.434, 1.821, and 3.06 for 10, 20, and 30 mg l^{-1}, respectively, implying that values of C were directly proportional to the surface adsorption of naphthalene in the rate-controlling step. The intraparticle diffusion rate constant, K_{id}, values were 0.12, 0.172, and 0.246, showing that $K_{id,}$ increased with concentration. Intraparticle diffusion becomes the sole rate-limiting step if the plot is linear and passes through the origin.[59] This study deviated from this condition, thus, intraparticle diffusion is not the sole rate-limiting step. The R^2 value obtained reduced with increasing concentration.

3.12 Error analysis for the kinetic models

It was found that the $SSE_{(pseudo\text{-}first\text{-}order)}$ value for the effect of concentration ranged between 0.017 and 0.89, while the value obtained for the pseudo-second-order ranged between 0.260 and 0.054. $ARE_{(pseudo\text{-}first\text{-}order)}$ value for the effect of concentration was greater than 9 %, while $ARE_{(pseudo\text{-}second\text{-}order)}$ value for the same factor was less than 4 % (Table 8). Therefore, the pseudo-second order model better predicts the adsorption of naphthalene on AWEPs than the pseudo-first order model.

Table 9 – SSE and ARE values for kinetic models

Kinetic model	Concentration / mg l^{-1}	SSE	ARE / %
pseudo-first order	10	0.0107	2.0366
	15	0.8850	9.1689
	20	0.5698	9.6227
pseudo-second order	10	0.0260	3.1737
	15	0.0250	1.5435
	20	0.0554	1.5028

4 Conclusion

This research successfully demonstrated the suitability of expanded polystyrene waste (WEPs) products as an effective adsorbent. The activant (acetylene) used improved the

surface characteristics of the AWEPs, and this influenced its adsorptive properties, particularly for the removal of naphthalene from aqueous solution. The adsorption process was chemically driven, as suggested by the fitness of the data generated to Dubinin-Radushkevich isotherm and pseudo-second-order kinetic models. This, therefore, opens more opportunities to explore the WEPs for the adsorption of organic pollutants from aqueous solution and real-life wastewater.

List of abbreviations and symbols

a_k – Khan model exponent
b_k – Khan constant
A – Temkin isotherm constant
ANOVA – analysis of variance
ARE – average relative error at monolayer coverage
AWEPS – acetylated waste expanded polystyrene
b – heat of adsorption constant
B – Temkin isotherm constant
BET – Brannuer–Emmet–Teller method
d – interlayer spacing, m
DOE – design of experiment
EPS – expanded polystyrene
FTIR – Fourier transform infrared spectroscopy
H – standard enthalpy, J mol^{-1}
h – initial adsorption rate as $t \rightarrow 0$, mg g^{-1} min^{-1}
IMR – impregnation ratio
K_1 – rate constant of pseudo-first order adsorption, 1/min
K_2 – rate constant of the pseudo-second, g mg^{-1} min^{-1}
k_{diff} – rate constant for intraparticle diffusion, m g^{-1} min^{-1}
k_F – Freundlich constant
K_L – free energy of adsorption constant
MBN – methylene blue number
MW – microwave
n – Hill coefficient of binding interaction of the adsorbate
OFAT – one factor at a time
PAHs – polycyclic aromatic hydrocarbons
q_e – adsorption capacity at equilibrium, mg g^{-1}
q_m – maximum adsorption capacity, mg g^{-1}
q_s – theoretical isotherm saturation capacity, mg g^{-1}
q_t – adsorption capacity at time t, mg g^{-1}
r – inverse power of distance from the surface, m^{-1}
R – universal gas constant, J mol^{-1} K^{-1}
RE – removal efficiency
RSM – response surface methodology
SSE – sum of square error
T – absolute temperature, K
V – volume, dm^3, cm^3
WEPS – waste expanded polystyrene
ΔG – change in Gibbs free energy, J mol^{-1}
ΔS – standard entropy change, J K^{-1}
β – free energy of adsorption *per* mole, KJ^2 mol^2
ε – Polanyi potential, J mol^{-1}
γ_e – equilibrium concentration, mg l^{-1}
γ_o – adsorbate initial concentration, mg l^{-1}
θ – degree of surface coverage

References
Literatura

1. *X. M. Xiao, F. Tian, Y. J. Yan, Z. S. Wu*, Adsorption behaviour of pyrene from onto coal based activated carbons prepared by microwave activation, J. Shihezi Univ. **32** (2014) 485–490.
2. *Q. Chen, T. Zheng, B. Bassig, Y. Cheng, B. Leadener, S. Lin, T. Holford, J. Qiu, Y. Zheng, K. Shi, Y. Zhu, J. Niu, Y. Li, H. Guo, X. Hu, Y. Jin*, Prenatal exposure to polyaromatic hydrocarbons and birth weight in China, Open J. Air Pollut. **3** (2014) 100–110, doi: https://doi.org/10.4236/ojap.2014.34010.
3. *S. S. Cai, J. A. Syage, K. A. Hanold, M. P. Balogh*, Ultra-performance liquid chromatography atmospheric pressure photoionization tandem mass spectrometry for high-sensitivity and high throughput analysis of U.S. Environmental Protection Agency 16 priority pollutants polynuclear aromatic hydrocarbons, Anal. Chem. **81** (2009) 2123–2128, doi: https://doi.org/10.1021/ac802275e.
4. *K. Edvinas, M. Dainius, S. V. Ruta, C. Darius, P. Tedas, K. Violeta, S. Inga, K. Linas*, Characterization of particulate and vapor phase polycyclic aromatic hydrocarbons in indoor and outdoor air of primary schools, Atmos. Environ. J. **82** (2014) 298–306, doi: https://doi.org/10.1016/j.atmosenv.2013.10.042.
5. *S. M. Yakout, A. A. Daifullah, S. A. El-Reefy*, Adsorption of Naphthalene, Phenanthrene, and Pyrene from Aqueous Solution Using Low-Cost Activated Carbon Derived from Agricultural Waste, J. Adsorpt. Sci. Technol. **31** (2013) 334–658, doi: https://doi.org/10.1260/0263-6174.31.4.293.
6. *R. J. Krupadam, M. S. Khan, S. R. Wate*, Removal of Probable Human Carcinogenic Polycyclic Aromatic Hydrocarbons from Contaminated Water Using Molecularly Imprinted Polymer, Water Res. **44** (2010) 681–688, doi: https://doi.org/10.1016/j.watres.2009.09.044.
7. *R. Quiroz, J. O. Grimalt, P. Fernandez*, Toxicity assessment of polycyclic aromatic hydrocarbons in sediments from European high mountain lakes, Ecotoxicol. Environ. Saf. **73** (2010) 559–1564, doi: https://doi.org/10.1016/j.ecoenv.2009.12.030.
8. *A. O. Alade, O. S. Amuda, T. J. Afolabi, A. A. Okoya*, Adsorption of Naphthalene onto Activated Carbons Derived from Milk Bush Kernel Shell and Flamboyant Pod, J. Environ. Chem. Ecotoxicol. **4** (2012) 124–132, doi: https://doi.org/10.5897/JECE11.041.
9. *A. A. Olajiire, A. O. Alade, A. A. Adejare, O. M. Olabemiwo*, Distribution of Polycyclic aromatic hydrocarbons in surface soils and water from the vicinity of Agbabu bitumen field of southwestern Nigeria, J. Environ. Sci. Health A **42** (2007) 1043–104, doi: https://doi.org/10.1080/10934520701418474.
10. *F. Murilo, T. Luna, C. B. Araujo, B. V. Carolina, J. Ivanildo, Jr. Silva, C. S. Diana, L. Celio, Jr. Cavalcante*, Adsorption of

Naphthalene and Pyrene from Isooctane Solutions on Commercial Activated Carbons, J. Environ. Sci. **17** (2011) 937–947, doi: https://doi.org/10.1007/s10450-011-9372-0.

11. *L. Monser, N. Adhoum*, Modified Activated Carbon for the Removal of Copper, Zinc, Chromium, and Cyanide from Wastewater, J. Sep. Purif. Technol. **26** (2002) 137–146, doi: https://doi.org/10.1016/S1383-5866(01)00155-1.
12. *A. Daifullah, B. Girgis, H. Gad*, Utilization of Agro-Residues (Rice-Husk) in Small Wastewater Treatment Plans, J. Waste Manag. **11** (2003) 1723–1731, doi: https://doi.org/10.1016/S0167-577X(02)01058-3.
13. *L. Seifi, A. Torabian, H. Kazemian, G. N. Bidhendi, A. A. Azimi, S. Nazmara, M. Alimohammadi*, Adsorption of BTEX on Surfactant Modified Granulated Natural Zeolite Nanoparticles: Parameters Optimizing by Applying Taguchi Experimental Design Method, J. Water Air Soil Pollut. **39** (2011) 939–948, doi: https://doi.org/10.1002/clen.201000390.
14. *F. Yu, J. Ma, Y. Wu*, Adsorption of Toluene, Ethylbenzene, and Xylene Isomers on Multi-Walled Carbon Nanotubes Oxidized by Different Concentration of NaOCl, J. Environ. Technol. **3** (2011) 320–329, doi: https://doi.org/10.1007%2Fs11783-011-0340-4.
15. *Y. Zhao, H. Zhang, P. Wang, F. Xue, Z. Ye, Y. Zhang, Y. Tang*, Tailoring the Morphology of MTW Zeolite Mesocrystals: Intertwined Classical/Non-Classical Crystallization, J. Chem. Mater. **19** (2017) 1058–1062, doi: https://doi.org/10.1021/acs.chemmater.6b03813.
16. *H. Nourmoradi, M. Nikaeen, H. H. Khiadani*, Removal of Benzene, Toluene, Ethylene, Chem. Eng. J. **191** (2012) 341–348, doi: https://doi.org/10.1016/j.cej.2012.03.029.
17. *L. Touyz*, Naphthalene Mothballs: A Silent Killer, NOVA publisher, NY11788, USA, 2014.
18. *C. H. Micheal*, Fact sheet on Naphthalene, Cancer Association of South Africa, 2015.
19. *E. Ayranci, O. Duman*, Structural Effects on the Interactions of Benzene and Naphthalene Sulfonates with Activated Carbon Cloth during Adsorption from Aqueous Solutions, Chem. Eng. J. **156** (2010) 70–76, doi: https://doi.org/10.1016/j.cej.2009.09.038.
20. *S. E. Agarry, M. O. Aremu*, Batch Equilibrium and Kinetic Studies of Simultaneous Adsorption and Biodegradation of Naphthalene by Orange Peels Immobilized *Pseudomonas Aeruginosa* NCIB 950, J. Bioremed. Biodegrad. **3** (2012) 138, doi: https://doi.org/10.9734/BBJ/2012/902.
21. *X. Ge, F. Tian, Z. Wu, Y. Yan, G. Cravotto, Z. Wu*, Adsorption of Naphthalene from Aqueous Solution on Coal-Based Activated Carbon Modified by Microwave Induction: Microwave Power Effects, Chemical Engineering, and Processing, J. Process Intens. **91** (2015) 57–77, doi: https://doi.org/10.1016/j.cep.2015.03.019.
22. *E. I. Osagie, C. N. Owabor*, Adsorption of Naphthalene on Clay and Sandy Soil from Aqueous Solution, Adv. Chem. Eng. Sci. **5** (2015) 345–351, doi: https://doi.org/10.4236/aces.2015.53036.
23. *G. Karthikeyan, S. Meenakshi, B. V. Apparao*, Water Engineering and Development Centre 20, 1994.
24. *N. Chaukura, W. Gwenzi, T. Bunhu, D. T. Ruziwa, I. Pumure*. Potential Uses and Value-Added Products Derived from Waste Polystyrene in Developing Countries: A review, J. Res. Conserv. Recyc. **107** (2015) 157–165, doi: https://doi.org/10.1016/j.resconrec.2015.10.031.
25. *A. Kan, R. Demirboga*, A New Technique of Processing for Waste-Expanded Polystyrene Foams as Aggregates, J. Mater. Process. Technol. **209** (2009) 2994–3000, doi: https://doi.org/10.1016/j.jmatprotec.2008.07.017.
26. *W. Gwenzi, D. Ruziwa, N. Chaukura, I. Pumure*, Removal of Zn^{2+} and Pb^{2+} Ions from Aqueous Solution using Sulphonated Waste Polystyrene, J. Environ. Chem. Eng. **3** (2015) 2528–2537, doi: https://doi.org/10.1016/j.jece.2015.08.006.
27. *J. Huang, X. Y. Yin, J. Y. Yang, M. L. Guo*, Solid Protonic Acids and Luminescent Carbon Dots Derived from Waste Expanded Polystyrene, J. Mater. Lett. **117** (2013) 112–115, doi: https://doi.org/10.1016/j.matlet.2013.11.104.
28. *A. N. Siyal, S. Q. Memon, S. Parveen, A. Soomro, M. I. Khaskheli, M. Y. Khuhawar*, Chemical Recycling of Expanded Polystyrene Waste: Synthesis of Novel Functional Polystyrene-Hydrazone Surface for Phenol Removal, J. Chem. **2** (2013) 1020–1035, doi: https://doi.org/10.1155/2013/842435.
29. *F. D. Alsewailem, S. A. All*, Recycled Polymer/Clay Composites for Heavy-Metals Adsorption, J. Mater. Technol. **47** (2013) 525–529.
30. *D. Ruziwa, N. Chaukura, W. Gwenzi, N. Pumure*, Removal of Zn^{2+} and Pb^{2+} ions from aqueous solution using sulphonated waste polystyrene, J. Environ. Eng. **11** (2015) 1135–1176, doi: https://doi.org/10.1016/j.jece.2015.08.006.
31. *O. Alabi, A. O. Alade, T. J. Afolabi*, Process optimization of adsorption of Cr (VI) on adsorbent prepared from Bauhinia rufescence pod by Box-Behnken Design, J. Sep. Sci. Technol. **55** (2020) 47–60, doi: https://doi.org/10.1080/01496395.2019.1577436.
32. *B. Jenkins, L. Baxter, T. Miles, T. Miles*, Combustion Properties of Biomass, J. Fuel Process. Technol. **54** (1998) 17–46, doi: https://doi.org/10.1016/S0378-3820(97)00059-3.
33. *O. A. Ekpete, M. Horsfall*, Kinetic Sorption Study of Phenol onto Activated Carbon Derived from Fluted Pumpkin Stem Waste (*Telfairia Occidentalis Hook. F*), J. Eng. Appl. Sci. **6** (2011) 43–49.
34. *E. Fuente, J. A. Menendez, M. A. Dyes, D. Sau'rez, M. A. Montes-Moran*, Infrared Spectroscopy of Carbon Materials: A Quantum Chemistry Study of Model Compounds, J. Phys. Chem. **1** (2003) 15–24, doi: https://doi.org/10.1021/jp027482g.
35. *Z. Lin, C. Guan, L. Huang, W. Wang, Q. Ling, C. Zhao*, Catalysis Studies of Microreticular Polystyrene Cation-exchange Resin with Terminal Perfluoroalkanesulfonic acids, J. Chin. Chem. Soc. **60** (2012) 261–266, doi: https://doi.org/10.1002/jccs.201200431.
36. *D. Krishna, R. Padma Sree*, Artificial Neural Network and Response Surface Methodology Approach for Modeling and Optimization of Chromium (VI) Adsorption from Waste Water using Ragi Husk Powder, Ind. Chem. Eng. **55** (3) (2013), doi: https://doi.org/10.1080/00194506.2013.829257
37. *I. O. Okeowo, E. O. Balogun, A. J. Ademola, A. O. Alade, T. J. Afolabi, E. O. Dada, A. G. Farombi*, Adsorption of Phenol from Wastewater Using Microwave-Assisted Ag–Au Nanoparticle-Modified Mango Seed Shell-Activated Carbon, Int. J. Environ. Res. **14** (2020) 215–233, doi: https://doi.org/10.1007/s41742-020-00244-7.
38. *S. Saygideger, O. Gulnaz, E. S. Istifli, N. Yucel*, Adsorption of Cd(II), Cu(II) and Ni(II) ions by *Lemna minor* L.: effect of physicochemical environment, J. Hazard. Mater. **126** (2005) 96–104. doi: https://doi.org/10.1016/j.jhazmat.2005.06.012.
39. *M. E. Argun, S. Dursun*, A New Approach to Modification of Natural Adsorbent for Heavy Metal Adsorption, J. Biores. Technol. **99** (2008) 2516–2527, doi: https://doi.org/10.1016/j.biortech.2007.04.037.
40. *O. S. Bello, M. A. Ahmad*, Response Surface Modeling and Optimization of Remazol Brilliant Blue Reactive Dye Re-

moval Using Periwinkle Shell-Based Activated Carbon, J. Sep. Sci. Technol. **46** (2011) 2367–2379, doi: https://doi.org/10.1080/01496395.2011.595756.

41. *N. A. Elnasri, M. A. Elsheik, M. A. Eltayeb*, Physico-Chemical Characterization and Freundlich Isotherm of Adsorption of Fe(II) from Aqueous Solution by Using Activated Carbon Prepared from Doum Fruit Waste, Arch. Appl. Sci. Res. **5** (2013) 149–158.
42. *A. O. Dada, J. O. Ojediran, A. P. Olalekan*, Sorption of Pb^{2+} from Aqueous Solution unto Modified Rice Husk : Isotherms Studies, J. Adv. Phys. Chem. **16** (2013) 225–286, doi: https://doi.org/10.1155/2013/842425.
43. *A. Adeleh, M. K. Ali, S. Farad,* A Kinetic and Thermodynamic Study of Methylene Blue Removal from Aqueous Solution by Modified Montmorillonite, J. Appl. Res. Water Wastewater **4** (2015) 150–155.
44. *M. Auta, B. H. Hameed*, Acid modified local clay beads as an effective low-cost adsorbent for dynamic adsorption of methylene blue, J. Ind. Eng. Chem. **19** (2013) 1153–1161, doi: https://doi.org/10.1016/j.jiec.2012.12.012.
45. *S. Chowdhury, P. D. Saha*, Artificial neural network (ANN) modeling of adsorption of methylene blue by NaOH-modified rice husk in a fixed-bed column system, Environ. Sci. Pollut. Res. **20** (2013) 1050–1058, doi: https://doi.org/10.1007/s11356-012-0912-2.
46. *Sh. Shahmohammadi-Kalalagh, H. Babazadeh*, Isotherms for the Sorption of Zinc and Copper onto Kaolinite Comparison for Various Error Functions, Int. J. Environ. Sci. Technol. **11** (2014) 111–118, doi: https://doi.org/10.1007%2Fs13762-013-0260-x.
47. *M. Zbair, M. Bottlinger, R. Brahmi, A. Ainassaari, M. Pirilä, A. Drif, R. L. Keiski, S. Ojala, M. Bensite*, Toward new benchmark adsorbents: preparation and characterization of activated carbon from argan nutshell for bisphenol A removal, Environ. Sci. Pollut. Res. **25** (2018) 1869–1882, doi: https://doi.org/10.1007/s11356-017-0634-6.
48. *Z. Fu, J. Jia, J. Li, C. Liu*, Transforming Waste Expanded Polystyrene Foam into Hyper-Crosslinked Polymers for Carbon dioxide Capture and Separation, J. Chemi. Eng. **323** (2017) 557–564, doi: https://doi.org/10.1016/j.cej.2017.04.090.
49. *C. O. Ania, B. Carbal, J. B. Parra, J. J. Pis*, Importance of the Hydrophobic Character of Activated Carbon on the Removal of Naphthalene from the Aqueous Phase, J. Adsorpt. Sci. Technol. **25** (2007), doi: https://doi.org/10.1260/026361707782398164.
50. *J. Yang, M. Yu, W. Chen*, Adsorption of hexavalent chromium from aqueous solution by activated carbon prepared from longan seed: kinetics, equilibrium, and thermodynamics, J. Ind. Eng. Chem. **21** (2015) 414–422, doi: https://doi.org/10.1016/j.jiec.2014.02.054.
51. *M. Rai, G. Shahi, V. Meena, R. Meena, S. Chakraborty, B. Rai, R. Singh*, Removal of hexavalent chromium Cr (VI) using activated carbon prepared from mango kernel activated with H_3PO_4, J. Res. Effic. Technol. **2** (2016) 63–70, doi: https://doi.org/10.1016/j.reffit.2016.11.011.
52. *S. Yildiz*, Kinetic, and Isotherm Analysis of Cu(Ii). Adsorption onto Almond Shell (*Prunus dulcis*), J. Ecol. Chem. Eng. **24** (2017) 87–106, doi: https://doi.org/10.1515/eces-2017-0007.
53. *A. Inyinbor, F. Adekola, G. Olatunji*, Kinetics, and isothermal modeling of liquid-phase adsorption of Rhodamine B onto urea modified Raphia hookerie fruit epicarp, J. Water Res. Ind. **15** (2016) 14–27, doi: https://doi.org/10.1007/s13201-016-0471-7.
54. *B. V. Carla, L. B. Allen, P. M. Cicero, C. A. Ari, S. D. Francisco, C. G. V. Luiz, B. A. F. Pierre, F. N. Ronaldo*, Adsorption of Polycyclic Aromatic Hydrocarbon from Aqueous Solutions by Modified Periodic Mesoporous Organosilica, J. Colloid Interface Sci. **357** (2011) 466–473, doi: https://doi.org/10.1016/j.jcis.2011.02.013.
55. *H. Hammud*, Biosorption Studies of Methylene Blue by Mediterranean Algae Carolina and Its Chemically Modified Forms. Linear and Nonlinear Models Prediction Based on Statistical Error Calculations, Int. J. Chem. **3** (2011) 147–163, DOI: https://doi.org/10.5539/ijc.v3n4p147.
56. *C. Chang, C. Chang, K. Chen, W. Tsai, J. Shie, Y. Chen*, Adsorption of Naphthalene on Zeolite from Aqueous Solution, J. Colloid Interface Sci. **277** (2004) 29–34, doi: https://doi.org/10.1016/j.jcis.2004.04.022.
57. *H. Gupta, B. Gupta*, Adsorption of Polycyclic Aromatic Hydrocarbon on Banana Peel Activated Carbon, J. Desal. Water Treat. **57** (2015) 9498–9509, doi: https://doi.org/10.1080/19443994.2015.1029007.
58. *M. Matouq, N. Jildeh, M. Qtaishat, M. Hindiyeh, M. Al Syouf*, The Adsorption Kinetics and Modelling for Heavy Metals Removal from Wastewater by Moringa Pods, J. Environ. Chem. Eng. **3** (2015) 775–784, doi: https://doi.org/10.1016/j.jece.2015.03.027.
59. *B. Das, N. K. Mondai, R. Bhaumik, P. Roy*, Insight into Adsorption Equilibrium, Kinetics and Thermodynamics of Lead onto Alluvial Soil, J. Environ. Sci. Technol. **11** (2014) 1101–1114, doi: https://doi.org/10.1007%2Fs13762-013-0279-z.

SAŽETAK

Recikliranje ekspandiranog polistirena kao učinkovitog adsorbensa naftalena iz vodene otopine

Oluwayemisi Christiana Taiwo,[a,b] *Tinuade Jolaade Afolabi*,[a,b] *Funmilayo Nihinlola Osuolale*,[a] *Ayobami Olu Ajani*,[a] *Olufunmilayo Abiola Aworanti*,[a] *Olabanji Raphael Ogunleye*,[a,b] and *Abass Olanrewaju Alade*[a,b,c*]

Šaržni faktori procesa adsorpcije [vrijeme kontakta (20 – 150 min), doziranje adsorbenta (0,5 – 1,5 g), koncentracija adsorbata (5–30 mg l^{-1}) i brzina miješanja (100–250 min^{-1})] optimizirani su na temelju D-optimalnog dizajna primjenom metodologije odzivne površine (RSM) programa *Design-Expert (7.6.8)* za uklanjanje naftalena iz vodene otopine pomoću adsorbenta razvijenog iz acetiliranog otpadnog ekspandiranog polistirena (AWEP). Ostvareni maksimalni adsorpcijski kapacitet (5,6608 mg g^{-1}) dobro je prilagođen izotermi Dubinin-Radushkevich (R^2 = 0,9949). SSE (< 0,05) i ARE (< 4,0 %) označili su pseudo-drugi red kao najprikladniji model. Ovo istraživanje pokazalo je učinkovitost WEP-a za uklanjanje naftalena iz vodene otopine.

Ključne riječi
Adsorpcija, D-optimalnost, naftalen, otpadni ekspandirani polistiren

[a] *Department of Chemical Engineering, Ladoke Akintola University of Technology, Ogbomoso, Nigerija*
[b] *Bioenvironmental, Water and Engineering Research Group, (BWERG), Ladoke Akintola University of Technology Ogbomoso, Nigerija*
[c] *Science and Engineering Research Group, (SEARG), Ladoke Akintola University of Technology Ogbomoso, Nigerija*

Izvorni znanstveni rad
Prispjelo 25. prosinca 2020.
Prihvaćeno 26. lipnja 2021.